

# Unveiling the Modification of Esterase-like Activity of Serum Albumin by Nanoplastics and Their Cocontaminants

Durgalakshmi Rajendran and Natarajan Chandrasekaran\*

Cite This: *ACS Omega* 2023, 8, 43719–43731

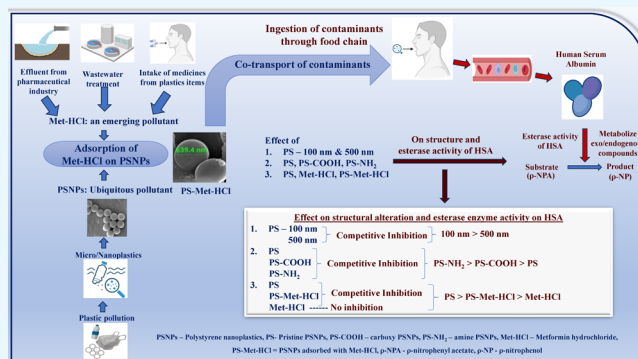
Read Online

ACCESS |

Metrics &amp; More

Article Recommendations

**ABSTRACT:** Nanoplastics and other cocontaminants have raised concerns due to their widespread presence in the environment and their potential to enter the food chain. The harmful effects of these particles depend on various factors, such as nanoparticle size, shape, surface charge, and the nature of the cocontaminants involved. On entering the human body, human serum albumin (HSA) molecules bind and transport these particles in the blood system. The esterase-like activity of HSA, which plays a role in metabolizing drug/toxic compounds, was taken as a representative to portray the effects of these particles on HSA. Polystyrene nanoplastics (PSNPs) with different surface functionalization (plain (PS), amine (PS-NH<sub>2</sub>), and carboxy (PS-COOH)), different sizes (100 and 500 nm), and PS with cocontaminant metformin hydrochloride (Met-HCl), a widely used antidiabetic drug, were investigated in this study. Fluorescence emission spectra of HSA revealed that PS-NH<sub>2</sub> exhibits a greater effect on protein conformation, smaller NPs have a greater influence on protein structure than larger NPs, and Met-HCl lowers PSNPs' affinity for HSA by coating the surface of the NPs, which may result in direct NP distribution to the drug's target organs and toxicity. Circular dichroism spectra also supported these results in terms of secondary structural changes. Esterase activity of HSA was inhibited by all the particles (except Met-HCl) by competitive inhibition as concluded from constant  $V_{\max}$  and increasing  $K_m$ . Greater reduction in enzyme activity was observed for PS-NH<sub>2</sub> among functionalizations and for 100 nm PS among sizes. Furthermore, Met-HCl lowers the inhibitory impact of PSNPs on HSA since the drug binds weakly to HSA, and so they can serve as a vector delivering PSNPs to their target organs, resulting in serious implications.



## 1. INTRODUCTION

Plastic pollution, such as plastic fragments (mesoplastics, macroplastics, microplastics: 1  $\mu\text{m}$  to 5 mm and nanoplastics: < 100 nm) formed from plastic bottles, bags, and packaging, has recently attracted most to public, policy, and research interest.<sup>1</sup> Through consumption, they enter the food chain and may have an impact on ecosystems at all levels.<sup>2</sup> Additionally, by adsorbing various copollutants on their surfaces, such as heavy metals, organic pollutants, and medicinal chemicals, nanoplastics serve as vectors for the transportation of other copollutants.<sup>3</sup> Polystyrene nanoplastics (PSNPs) are a significant representative of nanoplastics that get degraded from widely used disposable plates, tea cups, and so forth and have been extensively studied for their toxicity to all species.<sup>4</sup> Scientific studies have proved that polystyrene nanoplastics (PSNPs) adsorb a wide range of environmental contaminants such as pharmaceuticals (oxytetracycline<sup>5</sup> and ciprofloxacin<sup>6</sup>), pesticides (fipronil,<sup>7</sup> triadimenol (TRI), myclobutanil (MYC), and hexaconazole (HEX)),<sup>8</sup> POPs (polychlorinated biphenyls (PCBs), polycyclic aromatic hydrocarbons (PAHs), and dichlorodiphenyltrichloroethane (DDT)<sup>9</sup>), and heavy metals

(arsenic<sup>10</sup>). However, the adsorption of these substances depends on various factors such as the characteristics of the plastics (particle size, surface area/volume, surface charge, etc.<sup>11</sup>) and chemical interfaces, such as van der Waals bonds, hydrophobic interactions, or intraparticle diffusion.<sup>12</sup> Other polymers also have similar physiochemical properties as polystyrene<sup>13</sup> such as nonpolar nature (polyethylene (PE), polypropylene (PP)), amorphous structure (polyvinyl chloride (PVC)), and a glass-transition temperature of  $-90$  °C (PVC).<sup>12</sup> These polymers comparatively adsorb the environmental copollutants (sulfamethoxazole on PE,<sup>14</sup> tris(2,3-dibromopropyl) isocyanurate and hexabromocyclododecanes on PP,<sup>15</sup> and tylosin on PP, PE, PS, and PVC<sup>16</sup>) as

Received: July 26, 2023

Accepted: September 29, 2023

Published: November 6, 2023



polystyrene. PVC<sup>6</sup> and PE<sup>17</sup> have the capacity to adsorb the hydrophilic drug, ciprofloxacin.

Recent studies of wastewater treatment plant (WWTP) effluent and surface water have found extremely high quantities of one such pharmaceutical pollutant: metformin hydrochloride (Met-HCl), an antidiabetic drug.<sup>18</sup> Our previous research highlighted the physical and chemical interactions involved in the adsorption of metformin hydrochloride (Met-HCl) on PSNPs. Adsorption mechanisms follow pseudo-second-order kinetics, intraparticle diffusion, and Langmuir isotherm, undertaking both physisorption (electrostatic attraction, van der Waal's interactions, and hydrogen bonds at different pH) and chemisorption between Met-HCl and PSNPs, as evidenced from the research.<sup>19</sup> Comparably, other emerging pollutants also adsorb on micronanoplastics (MNPs) (fipronil,<sup>7</sup> oxytetracycline,<sup>5</sup> pyrene,<sup>20</sup> etc.). Further, similar to Met-HCl, other hydrophilic compounds (antibiotics,<sup>6,17</sup> personal care products<sup>11</sup>) can also be adsorbed on MNPs. Several combined toxicity studies of nanoplastics and copollutants have been conducted on aquatic organisms,<sup>21–25</sup> mice models,<sup>26,27</sup> and cell lines.<sup>28,29</sup> However, only a few research studies have looked into how MNPs and associated cocontaminants affect the human circulatory system. Correspondingly, their combined impact on plasma protein, a major distributor of exogenous compounds in the human bloodstream, is indispensable to explore. Thus, in this study, the cocontaminant (Met-HCl)-adsorbed PSNPs on the enzyme activity of human serum albumin (HSA) were investigated, which can be extrapolated to other emerging pollutants.

The interaction between HSA and nanoplastics and the formation of their complex are termed a protein corona.<sup>30</sup> This protein corona is related to the environmental occurrence of biocorona or ecocorona between MNPs and other environmental contaminants (biomolecules, toxicants, etc.). MNPs can form corona extensively with a variety of different substances, including metal cations, inorganic anions, organic compounds, and biomolecules, due to their high surface area and significant binding affinity. These coronated compounds enter the food chain (marine plankton, fishes, higher organisms) and eventually enter humans causing several toxicities.<sup>31</sup> A number of plasma proteins had a potent affinity for NPs and generated multilayered corona ranging in size from 13 to 600 nm. The nonspecific protein–protein attraction used by the coronated NPs to attract one another eventually led to protein-induced coalescence in the NPs. From the protein's perspective, the contact led to denaturation and conformational alterations, which rendered the protein bioincompatible. In comparison to virgin NPs, coronated NPs with enhanced protein confirmation modifications had a greater genotoxic and cytotoxic effect on human blood cells (hemolysis, thrombocyte activation, etc.).<sup>32</sup>

HSA is perhaps the most explored serum albumin protein; it has a well-known structure with 585 amino acid residues and 17 disulfide bridges.<sup>33</sup> It has three homologous helical domains, with subdomains IIA and IIIA each having two unique ligand binding sites designated as site I and site II, respectively.<sup>34</sup> Any foreign particles entering the circulatory system are immediately exposed to serum albumins, which attach to them.<sup>35</sup> Drug or toxic material distribution and cell uptake and internalization are all influenced by plasma protein binding.<sup>31,36</sup> Strong protein binding inhibits high molecular protein–ligand complexes from traversing biological membranes, impairing metabolism, and renal clearance, which may

be a symptom of persistence and/or bioaccumulation.<sup>37</sup> HSA serves as a carrier protein for both endogenous and exogenous substances, facilitating the delivery of drugs, nutrients, hormones, fatty acids, and other molecules to specific organs. These actions assist the HSA's physiological actions in conserving homeostasis and aiding the transfer of vital compounds throughout the body. If the chemical is toxic, this interaction would result in structural and functional changes in the molecules, denaturing HSA and reducing its biological activity.<sup>38</sup>

HSA has a wide range of enzymatic properties, one such is “esterase activity”, which refers to HSA's capacity to hydrolyze or cleave ester linkages or form covalent bonds with ester substrates through specific amino acids, which produces alcohol and carboxylic acid.<sup>39</sup> These activities may be physiologically significant, such as the metabolism of drugs and other endogenous and exogenous substances, including toxic substances besides the detoxification of substances containing ester groups.<sup>40</sup> In some clinical circumstances, such as liver disorders, where alterations to HSA structure or binding qualities may affect its enzymatic activity, the esterase activity of HSA may be changed.<sup>41</sup> HSA-based biosensors have been developed as an application to detect ester-containing substances or to monitor enzymatic processes involving ester substrates.<sup>42</sup> It may also be useful in drug delivery systems, where ester bonds are exploited as cleavable linkers for the regulated release of medicines.<sup>43</sup> Drugs and pollutants may bind nonspecifically or specifically at Sudlow's sites I and II of HSA, potentially influencing its enzymatic function.<sup>44</sup> The binding of drugs or pollutants to HSA can have a substantial impact on their pharmacokinetics and pharmacodynamics, altering their distribution, metabolism, efficacy, safety, and toxicity.<sup>43</sup> These exogenous compounds inhibit the esterase activity of HSA by reversible or irreversible inhibition.<sup>45</sup> Reversible inhibition includes competitive (binding to the active site), uncompetitive (binding to the enzyme–substrate complex), and noncompetitive inhibition (binding a distinct site from the active site, inducing conformational changes, and affecting esterase activity), whereas irreversible inhibition occurs by strong covalent bonds.<sup>46</sup>

For evaluating the toxicological effects of pollutants on human health, it is essential to comprehend the potential inhibition of HSA's esterase activity. The precise mechanisms and effects of pollutant-induced inhibition (reversible or irreversible) on HSA's esterase activity will be ascertained through experimental characterization and kinetic analysis. In toxicology, if nanoplastics or other toxic agents bind to HSA in a competitive manner, the capacity of HSA to bind to ester-containing poisonous compounds may be compromised, which may result in a decline in the detoxification of harmful chemicals.<sup>39</sup> In recent times, the “Trojan horse effect” of nanoplastics (vectors for other copollutants in the food chain) has gained importance in assessing their combined toxicity. In the present research, the effect of different functionalized, sized, and cocontaminant (Met-HCl)-adsorbed PSNPs on the esterase enzyme activity of HSA was investigated. Understanding these abnormalities might shed light on the toxicokinetics and toxicodynamics of nanoplastics and their copollutant complex in the human body.

## 2. MATERIALS AND METHODS

**2.1. Chemicals Required.** Monodispersed plain polystyrene microspheres (PS) (mean diameter: 100 and 500 nm),

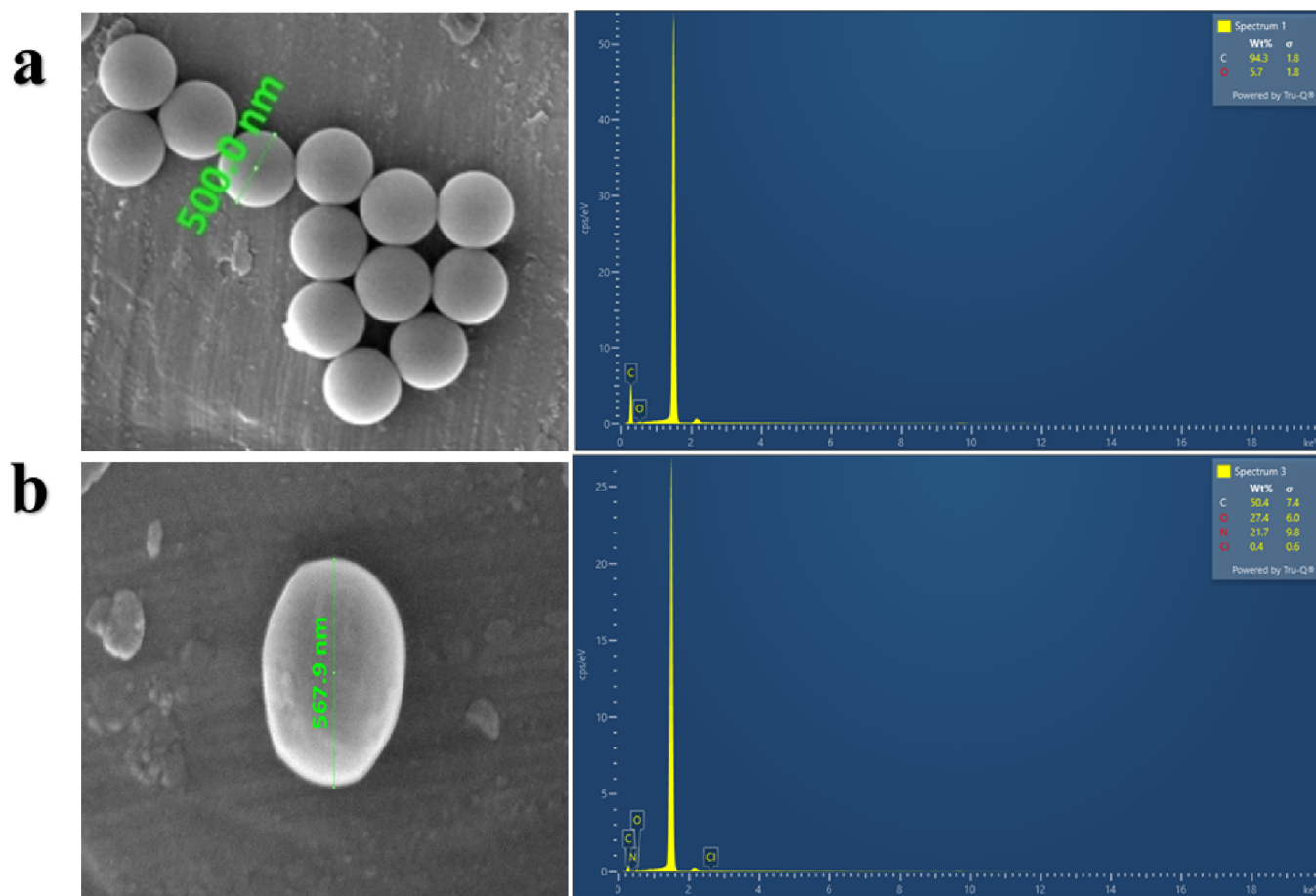


**Figure 1.** FE-SEM analysis: surface morphology with EDX spectra of (a) plain PSNPs and (b) Met-HCl-adsorbed PSNPs.

carboxylate polystyrene microspheres (PS-COOH) (100 nm), and amino polystyrene microspheres (PS-NH<sub>2</sub>) (100 nm) were acquired from Polysciences, Inc., USA. Using an ultrasonicator (VCX-750, Sonics & Materials, Inc., USA), microspheres of 10 g/L stock were dispersed in Milli-Q water. Metformin hydrochloride was procured from Hi-Media Laboratories, India. Human serum albumin (EC number: 274-272-6) was purchased from Sigma-Aldrich, USA, as a lyophilized powder. Freshly made phosphate buffer with a pH of 7.4 was used to make an HSA stock solution ( $1 \times 10^{-4}$  M) from which  $1 \times 10^{-5}$  M was made by dilution for the interaction investigations. There were three duplicates of each experiment.

**2.2. Field Emission Scanning Electron Microscopy (FESEM).** In order to observe the adsorption of Met-HCl on PSNPs, pristine PSNPs (10 mg/L, 500 nm) and PSNPs (10 mg/L) that had been exposed to Met-HCl (10 mg/L each) were held for shaking under conditions that encouraged maximum adsorption before being completely dehydrated using the ALPHA 1–2 LD plus freeze-dryer, manufactured by Martin Christ in Germany. Samples were analyzed for morphology under a field emission scanning microscope (Thermo Fisher FEI-Quanta 250 FEG, USA) operated at 20 kV acceleration voltage and a magnification of 50,000 $\times$ . Energy-dispersive X-ray spectroscopy (EDX) was used to measure the elemental compositions using a backscattered electron detection system. Before examination, the samples were lightly sputtered with gold.

**2.3. Fluorescence Quenching.** The specific intermolecular interactions between ligand and protein are extensively investigated using fluorescence spectroscopy as a primary spectroscopic approach.<sup>47</sup> Fluorescence emission spectra of a protein experience hypochromic effects (decrease in fluorescence intensity) as a result of intermolecular interactions such as energy transfer, electron rearrangement, ground-state complex formation, and excited-state collisions with ligands. Fluorescence quenching is the phrase used to describe such a decrease in emission intensity.<sup>48</sup>

An FP-8300 spectrofluorometer (JASCO, Japan) was used to record the fluorescence emission spectra. To find the emission spectra of experimental samples, the maximum excitation wavelength ( $\lambda_{ex}$ ), which was determined from UV–visible spectra to be 276 nm, was used.<sup>49</sup> The excitation and emission bandwidths were maintained at 2.5 and 5 nm for measurements of emission spectra between 280 and 400 nm at 310 K. A fixed concentration of HSA ( $1 \times 10^{-5}$  M) was combined with 50  $\mu$ g/mL concentrations of all the samples (PS: 100 and 500 nm, PS-COOH, PS-NH<sub>2</sub>, Met-HCl, Met-HCl-adsorbed PSNPs).

**2.4. Circular Dichroism Spectroscopy.** Circular dichroism (CD) spectra of HSA in the absence and presence of NPs were measured using a JASCO J-815 CD spectrophotometer. The absorbance was measured from 190 to 350 nm with a scanning speed of 100 nm/min. Secondary structural analysis was obtained by using the software from the JASCO manufacturer (Tokyo, Japan). A fixed concentration of HSA ( $1 \times 10^{-5}$  M) was combined with 50  $\mu$ g/mL concentrations of

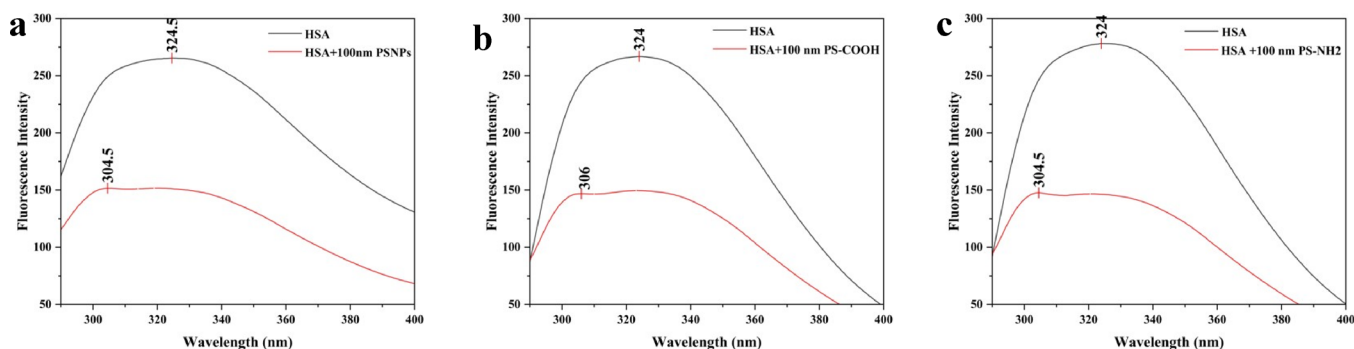


**Figure 2.** Fluorescence emission spectra of HSA on interaction with (a) PS, (b) PS-COOH, and (c) PS-NH<sub>2</sub>, [HSA] =  $1 \times 10^{-5}$  M, [PSNPs] = 0, 50  $\mu\text{g}/\text{mL}$ , pH 7.4,  $T = 310$  K.

all the samples (PS: 100 and 500 nm, PS-COOH, PS-NH<sub>2</sub>, Met-HCl, Met-HCl-adsorbed PSNPs).

**2.5. Effect on HSA's Esterase Activity.** Numerous enzyme activities, including esterase, RNA hydrolysis, antioxidant activity, lipid peroxidase, glucuronidase, and so forth are demonstrated by HSA.<sup>39</sup> To investigate the negative impact of pollutants on the enzyme activity of HSA, an esterase activity assay of HSA was carried out in the presence of those pollutants. The concept behind this test is to employ a UV-visible spectrophotometer fixed at 405 nm to measure the absorbance of  $\rho$ -nitrophenol, a yellow product that is produced when the substrate  $\rho$ -nitrophenyl acetate ( $\rho$ -NPA) is hydrolyzed by HSA.<sup>50</sup> This hydrolysis of  $\rho$ -NPA by HSA is termed its esterase-like activity. The substrate concentration of 0–800  $\mu\text{M}$  was utilized in this experiment. An increasing concentration of samples (0, 50, 100  $\mu\text{g}/\text{mL}$ ) (PS: 100 and 500 nm, PS-COOH, PS-NH<sub>2</sub>, Met-HCl, Met-HCl-adsorbed PSNPs) was incubated with a  $1 \times 10^{-5}$  M concentration of HSA. The interaction between HSA and samples was evaluated using the difference in absorbance in the presence and absence of PSNPs and subsequent reduction in HSA's enzyme activity.

The following kinetic parameters<sup>51</sup> were determined using enzyme kinetic calculations and the Michaelis–Menten equation:

$$V_0 = \frac{V_{\max}[S]}{K_m + [S]} \quad (1)$$

$$k_{\text{cat}} = \frac{V_{\max}}{E} \quad (2)$$

where  $V_0$  is the initial velocity of  $\rho$ -nitrophenol formation,  $V_{\max}$  is the maximum velocity of  $\rho$ -nitrophenol formation,  $[S]$  is the concentration of substrate,  $K_m$  is the Michaelis–Menten constant,  $k_{\text{cat}}$  is the kinetic parameter,  $E$  is the enzyme concentration.

To verify the parameters examined, a Lineweaver–Burk plot (double reciprocal plot) was also plotted between the inverse of velocity and the inverse of substrate concentration,  $\left\{\frac{1}{V_0} \text{ vs } \frac{1}{[S]}\right\}$ , in both the absence and presence of PSNPs.

$$\frac{1}{V_0} = \frac{K_m}{V_{\max}[S]} + \frac{1}{V_{\max}} \quad (3)$$

**2.6. Statistical Analysis.** The data reported throughout the entire article represent the mean values of results acquired from triplicate experiments carried out under the same circumstances, and descriptive statistics of mean and standard

deviation were used to calculate the results. The software suite OriginPro 2022b was used to process the data.

### 3. RESULTS AND DISCUSSION

**3.1. FESEM Confirming Adsorption of Pharmaceutical (Met-HCl) on PSNPs.** FESEM, which analyses the micro/nanostructure of particles using an electron beam,<sup>52</sup> can be used to determine the surface morphology of pristine PSNPs and PSNPs adsorbed with copollutant Met-HCl. Figure 1a,b, respectively, show FESEM images of plain PSNPs and PSNPs adsorbed with Met-HCl at 100,000 $\times$  magnification (scale bar 1  $\mu\text{m}$ ). The average size of plain PSNPs was observed to be  $500 \pm 10$  nm, whereas PSNPs adsorbed with Met-HCl were found to be  $>550$  nm using ImageJ software. It was also found that the PSNPs' surface morphology was consistently smooth before they interacted with the Met-HCl, but after adsorption, it changed to a nonuniform shape. Met-HCl had been adsorbed on PSNPs, as evidenced by these morphological alterations. An EDX spectrum was used to confirm the PSNPs' elemental constituents both before and after adsorption. A prominent nitrogen (21.7%) and chlorine (0.4%) peak emerged in the PSNPs after getting into contact with Met-HCl. Thus, EDX mapping demonstrated that Met-HCl had adsorbed to NPs.

Furthermore, Met-HCl adsorption on PSNPs was thoroughly investigated in our prior research,<sup>19</sup> which showed that at various solution pHs, Met-HCl adsorb on PSNPs by electrostatic attraction as well as other forces such as van der Waal interactions and hydrogen bonds. Adsorption kinetics revealed both pseudo-first- and second-order fit kinetic data, demonstrating both physisorption and chemisorption involvement in the adsorption process along with intraparticle diffusion. Met-HCl sorption on PSNPs was better explained by the Langmuir isotherm model, which also supports the monolayer coverage adsorption mechanism that was visible in the FESEM pictures. The chemical interaction between Met-HCl and PSNPs was also verified by Fourier transform infrared (FTIR) and high-resolution mass spectrometry (HRMS).

**3.2. Fluorescence Emission Spectra.** A fraction of internal protein motions can be studied using fluorescence spectroscopy since it possesses the sensitivity and time resolution needed. Due to the presence of the three intrinsic fluorophores phenylalanine (Phe), tryptophan (Trp), and tyrosine (Tyr) in HSA, external dye is not necessary for fluorescence studies.<sup>36</sup> These residues are crucial for the shift to the quaternary state that takes place after ligand binding.<sup>53</sup> Phenylalanine (Phe) has a very low quantum yield and a weak

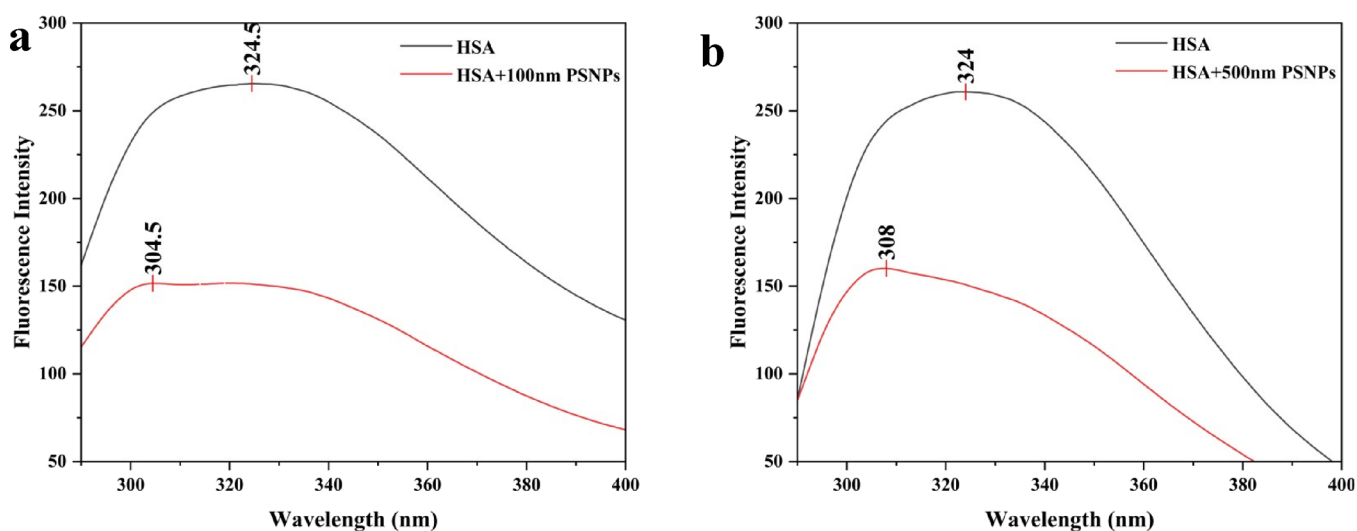


**Figure 3.** Fluorescence emission spectra of HSA on interaction with (a) PS-100 nm and (b) PS-500 nm,  $[HSA] = 1 \times 10^{-5}$  M,  $[PSNPs] = 0, 50$   $\mu\text{g/mL}$ ,  $\text{pH} = 7.4$ ,  $T = 310$  K.

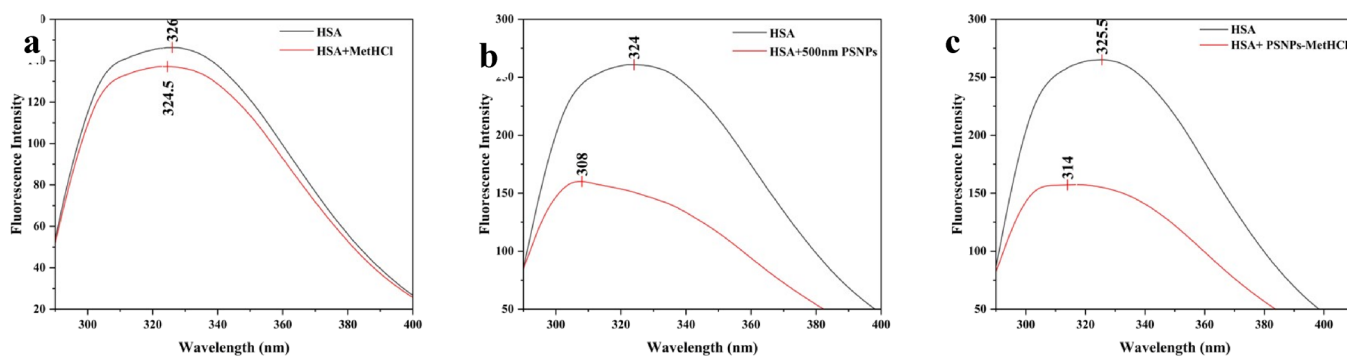


**Figure 4.** Fluorescence emission spectra of HSA on interaction with (a) Met-HCl, (b) PSNPS-500 nm, and (c) PSNPS-Met-HCl,  $[HSA] = 1 \times 10^{-5}$  M,  $[PSNPs] = 0, 50$   $\mu\text{g/mL}$ ,  $\text{pH} = 7.4$ ,  $T = 310$  K.

absorptivity, which limit its contribution to the intrinsic fluorescence of proteins. While the quantum yields of Tyrosine (Tyr) and Tryptophan (Trp) are comparable, leading to the hypothesis that Tyr and Trp are the prominent aromatic amino acid residues interacting with ligands.<sup>54</sup> It is projected that fluorophores will become more accessible to the polar environment as a result of the unfolding of the specific protein when a substance's emission intensity reduces.<sup>33</sup> Additionally, the HSA's lone tryptophan residue is notably helpful in binding tests.<sup>55</sup> Since spectrum shift is frequently employed to track dynamic and structural changes, variations in the intrinsic fluorescence of HSA can disclose a wealth of information. As a result, the interaction between HSA and exogenous ligands may be revealed by changes in the fluorescence emission spectrum.<sup>48</sup>

**3.2.1. Effect of Functionalized Nanoplastics on Quenching.** Studies had been done to determine how varied NP sizes and surface charges affected the structural changes in serum proteins.<sup>56–58</sup> However, they did not inquire how they affect the proteins' activities. This calls for a thorough investigation into how the surface charge (plain, amine, and carboxylated) and size (lowest: 100 nm, highest: 500 nm) of NPs affect the enzyme activity of HSA. The fluorescence emission spectra of HSA upon interaction with 50  $\mu\text{g/mL}$  of three distinct NPs, such as PS, PS-COOH, and PS-NH<sub>2</sub>, are shown in Figure 2a–c, respectively, at 310 K. Hypochromicity in all of the spectra

indicates that the protein is effectively quenched by contact, which implies that all three molecules have a significant impact on the milieu surrounding the intrinsic fluorophore, leading to fluorescence quenching. The quenching ability of nanoplastics was reported to be greatest in the sequence of PS-NH<sub>2</sub> > PS-COOH > PS: 47.41% > 43.98% > 43.1%. All of the interacted complexes (HSA+PS, HSA+PS-COOH, and HSA+PS-NH<sub>2</sub>) experienced a blue shift in the maximum emission wavelength ( $\lambda_{em} = 324$  nm), due to the fact that all NPs move toward the benzene end of the fluorophore residues of HSA, causing them to shift to shorter wavelengths,<sup>59</sup> which causes disorderliness in the position of the amino acid, which will be followed by unfolding of HSA.<sup>60</sup> In the PS-NH<sub>2</sub>-interacting complex, the emission spectrum showed a greater hypochromicity (19.5 nm) and hypochromicity (47.41%) simultaneously, indicating that amine-functionalized polystyrene NPs trigger stronger hydrophobicity surrounding aromatic amino acids than carboxy and plain polystyrene. A similar trend in the sequence of nanoplastic's effect was observed for human hemoglobin in our previous research.<sup>57</sup> The NPs themselves, however, have no discernible influence on the measured fluorescence signal since they do not exhibit fluorescence in the HSA emission range.

**3.2.2. Effect of Different Sized Nanoplastics on Quenching.** Figure 3a,b explores the change in emission of HSA when interacting with 100 and 500 nm PSNPs. Emission spectra of

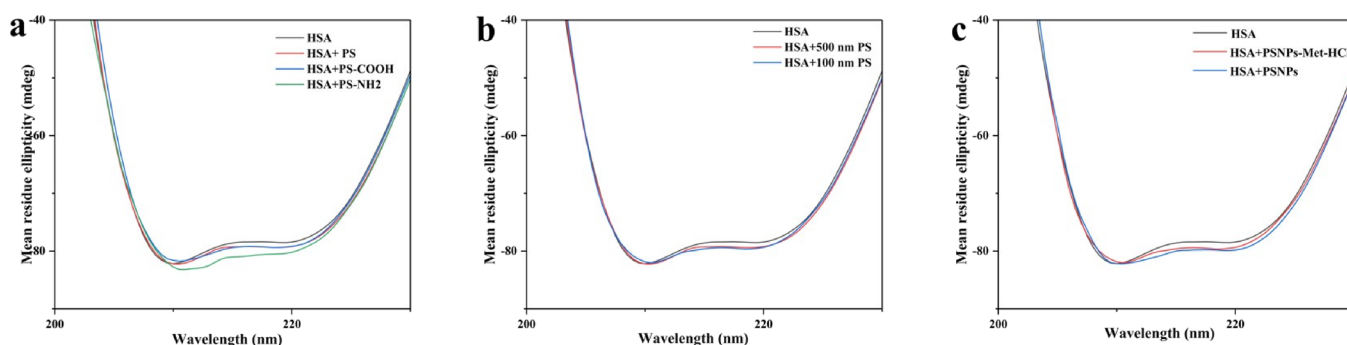


**Figure 5.** Circular dichroism spectra of HSA on interaction with functionalized (a) PSNPs, (b) different sized PSNPs, and (c) pristine PSNPs and PSNPs-Met-HCl, [HSA] =  $1 \times 10^{-5}$  M, [PSNPs] = 0, 50  $\mu\text{g/mL}$ .

**Table 1.** Secondary Structural Percentage of HSA Before and After Interaction with Various NPs

s.no	ligands	$\alpha$ -helix (%)	$\beta$ -antiparallel (%)	$\beta$ -parallel (%)	$\beta$ -turns (%)	others (%)
1	HSA	0.3	39.3	0	14.7	45.7
2	HSA+100 nm PS	0	38.7	0	14.3	47
3	HSA+PS-COOH	0	39.6	0	14.8	45.6
4	HSA+PS-NH <sub>2</sub>	0	41.1	0	14.3	44.6
5	HSA+500 nm PS	0	38.6	0	14.5	47
6	HSA+PSNPs-Met-HCl	0.2	38	0	14.7	47.2

HSA corona complexes with polystyrene NPs (50  $\mu\text{g/mL}$ ) of different diameters (100 and 500 nm) revealed hypochromicity in both spectra, showing that both sizes have a considerable impact on the environment surrounding the intrinsic fluorophore, resulting in fluorescence quenching. The quenching potential of nanoplastics was observed to be the most effective with the order of 100 nm PSNPs > 500 nm PSNPs: 43.1% > 42.15%. Both the complexes displayed a blue shift, with the largest shift observable with 100 nm PSNPs (16 nm), demonstrating that smaller NPs elicit the most notable conformational changes in the protein corona and create more hydrophobicity around fluorophores than bigger NPs. This has the effect of decreasing the quantum yield of fluorescence, increasing the energy loss through collisions and decreasing the fluorescence signals in the experimental system.<sup>61</sup> From the spectra results, the following conclusion can be made: smaller NPs (100 nm) usually having a large surface area-to-volume ratio increase the reactivity of the surface,<sup>62</sup> which can increase interaction with HSA. Regarding larger particles (500 nm), the small surface area-to-volume ratio weakens the interaction with protein.<sup>61</sup> This implies that smaller NPs are more likely than larger NPs to interfere with physiological processes that depend on proteins. Human hemoglobin showed a similar pattern in the order of the nanoplastic's effects.<sup>56</sup>

**3.2.3. Effect of Pharmaceutical-Adsorbed Nanoplastics on Quenching.** The emission spectra of HSA on the interaction with Met-HCl, PSNPs, and binary complex (Met-HCl-adsorbed PSNPs) at 310 K are portrayed in Figure 4a–c. The ligands had associated with HSA at or close to the fluorophore site, and quenching had taken place, as evidenced by a decrease in fluorescence intensity. All three spectra showed hypochromicity and hypsochromicity at the maximum emission wavelength ( $\lambda_{em}$ ) of HSA, with pristine PSNPs showing a significant quenching and shift (blue shift-16 nm) and Met-HCl by itself showing the least. The following order of ligands has the greatest influence on the milieu surrounding intrinsic fluorophores: PSNPs > binary complex > Met-HCl

(quenching percentage: 42.15% > 41.49% > 6.41%). Quenching and blue shift account for the increase in hydrophobicity near fluorophores.<sup>63</sup> In this instance, Met-HCl lessens the PSNPs' hydrophobic impact as evident from the reduction in a hypsochromic shift of HSA by 6 nm by covering the surface of PSNPs. Therefore, PSNPs' binding affinity for plasma protein is reduced when Met-HCl is adsorbed on their surface.

In our earlier study,<sup>19</sup> Met-HCl, PSNPs, and their complex were examined for their interactions with HSA in order to understand the effects of the complex on protein. The Stern–Volmer plot showed that the values of the Stern–Volmer constant  $K_{SV}$  and the quenching constant  $K_q$  values were considerably larger in the order of pristine PSNPs > binary complex > Met-HCl, suggesting that the binary complex quenches HSA less than pure PSNPs do. This is due to the fact that since Met-HCl covers the surface of PSNPs, it reduces the binding affinity of PSNPs with HSA, as they have negligible binding affinity with HSA. The thermodynamic investigation demonstrated that Met-HCl forms hydrophobic interactions with HSA, whereas PSNPs and complexes form hydrogen bonding interactions with HSA, which may explain why PSNPs and complexes have a higher binding affinity with HSA than Met-HCl. These findings show that the drug's low affinity for HSA determines the strength of the interaction between the protein and the drug-coated nanoplastics. Because of the decreased interaction strength, plasma protein binding is weakened, and Met-HCl may deliver PSNPs to their target organs, potentially causing organ damage. These spectra lead us to the conclusion that since the drugs are coating the surface of the NPs when nanoplastics are adsorbed with a pharmaceutical copollutant, their binding affinity with serum protein depends on that of the drug's binding affinity. If the medication has a lower affinity for binding, the complex will also bind less strongly to serum proteins and may be delivered straight to the drug's target cells, which could have more serious effects. If the drug has a higher affinity for binding, complex pollutants also attach to proteins more strongly,

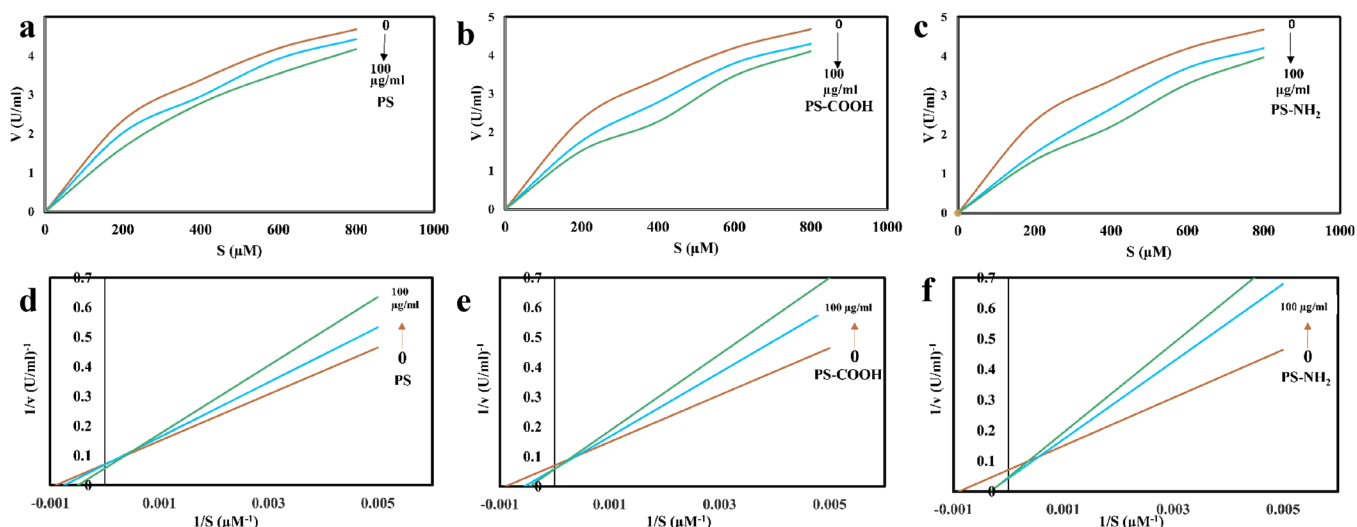


**Figure 6.** Michaelis–Menten plot: esterase enzyme activity of HSA on binding with (a) PS, (b) PS-COOH, and (c) PS-NH<sub>2</sub> NPs (0, 50, 100 µg/mL). Lineweaver–Burk plot ( $\frac{1}{v}$  vs  $\frac{1}{S}$ ): PS (d), PS-COOH (e), and PS-NH<sub>2</sub> (f). Straight lines represent the linear regression that fits scattered data points obtained at different substrate concentrations.<sup>39</sup>

**Table 2. Michaelis–Menten Parameters of HSA on Interaction with Increasing Concentration of Pollutants<sup>a</sup>**

s.no	NPs	concentration of pollutants (µg/mL)	$V_{max}$ (U/ml)	$K_m \times 10^3$ (µM)	$k_{cat} \times 10^3$ (S <sup>-1</sup> )
1	PS-100 nm	0	14.04 ± 0.019	1.10 ± 0.029	1.83 ± 0.032
2		50	14.40 ± 0.008	1.33 ± 0.003***	2.22 ± 0.004***
3		100	17.57 ± 0.056	2.03 ± 0.015***	3.38 ± 0.041***
4	PS-COOH	0	14.04 ± 0.053	1.10 ± 0.009	1.83 ± 0.012
5		50	16.66 ± 0.018	1.79 ± 0.020***	2.98 ± 0.000***
6		100	17.00 ± 0.026	2.17 ± 0.017***	3.63 ± 0.017***
7	PS-NH <sub>2</sub>	0	14.04 ± 0.053	1.10 ± 0.018	1.83 ± 0.014
8		50	22.88 ± 0.034	2.11 ± 0.000***	3.53 ± 0.002***
9		100	21.27 ± 0.026	2.50 ± 0.012***	4.16 ± 0.012***
10	PS-500 nm	0	14.04 ± 0.044	1.10 ± 0.010	1.83 ± 0.016
11		50	14.38 ± 0.008	1.28 ± 0.012***	2.13 ± 0.050***
12		100	13.98 ± 0.026	1.31 ± 0.023***	2.19 ± 0.005***
13	Met-HCl	0	14.04 ± 0.008	1.10 ± 0.025	1.83 ± 0.009
14		50	14.28 ± 0.024	1.12 ± 0.000 <sup>ns</sup>	1.87 ± 0.026 <sup>ns</sup>
15		100	14.51 ± 0.015	1.15 ± 0.021*	1.92 ± 0.014*
16	PSNPs-Met-HCl	0	14.04 ± 0.053	1.10 ± 0.026	1.83 ± 0.012
17		50	14.16 ± 0.032	1.16 ± 0.008*	1.93 ± 0.006*
18		100	13.55 ± 0.014	1.19 ± 0.011**	1.99 ± 0.007**

<sup>a</sup>\*\*\* $P < 0.005$ , \*\* $P < 0.01$ , \* $P < 0.05$ , ns: no significant difference in  $V_{max}$  (U/ml) values.

which could result in bioaccumulation influencing toxicokinetics/dynamics.

**3.3. Circular Dichroism Spectra.** CD spectroscopy was used to investigate the secondary structure of HSA both before and after it interacted with PS ligands, and their corresponding spectra were recorded (Figure 5a–c). Two negative bands at 208 and 220 nm may be seen in the CD spectra of HSA, which are indicative of the protein's  $\alpha$ -helix structure.<sup>64,65</sup> This  $\alpha$ -helical structure was found completely lost in all the interacted samples except with the PSNPs-Met-HCl complex (Table 1). PS-NH<sub>2</sub> showed a significant increase in both of the negative bands of HSA than carboxy and plain, with a slight shift toward increasing wavelength indicating there is a noticeable change in the ellipticity. Also, an increase in the percentage of  $\beta$ -antiparallel sheet and complete loss of  $\alpha$ -helix (Table 1) suggests that there are intermolecular hydrogen bonding rearrangements in HSA.<sup>32</sup> The secondary structure of HSA

following interaction with varying PS size shows variation in the spectra with the least significance. However, it was shown that a very slight change in the ellipticity indicates that a conformational change<sup>30</sup> is associated with the higher surface area-to-volume ratio of smaller NPs (100 nm). When comparing the effects of pristine PSNPs and the PSNPs-Met-HCl complex, pristine PSNPs show a larger impact and ellipticity change. The complex has less of an effect than PSNPs because the PSNPs' surface is covered by Met-HCl, which prevents them from attaching to HSA.

**3.4. Effect on Esterase Enzyme Activity.** HSA demonstrates significant physiological activity in the circulatory system due to its binding and catalytic effectiveness. This protein displays esterase-like activity, hydrolyzing esters, phosphates, and amides, which is usually impacted by structural alterations.<sup>66</sup> As a result, the effect of the foreign ligand on the HSA esterase activity must be investigated.

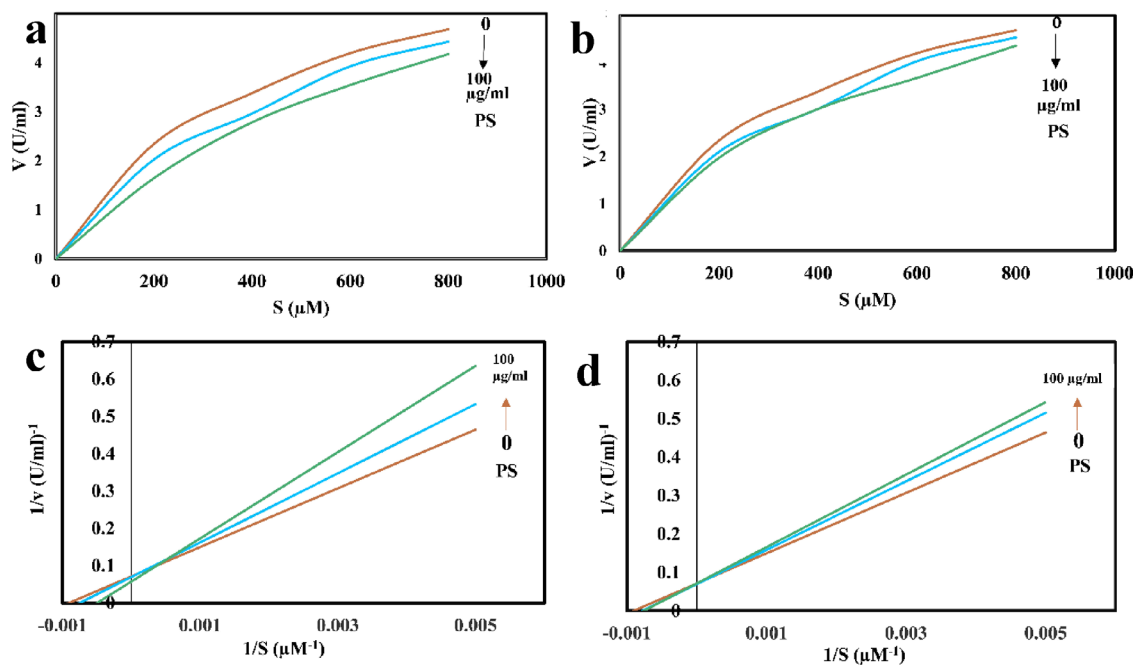


**Figure 7.** Michaelis–Menten plot: esterase enzyme activity of HSA on binding with (a) PS-100 nm and (b) PS-500 nm NPs (0, 50, 100  $\mu\text{g}/\text{mL}$ ). Lineweaver–Burk plot ( $\frac{1}{v}$  vs  $\frac{1}{S}$ ): (c) PS-100 nm and (d) PS-500 nm.

Notably, HSA demonstrates stereoselective esterase-like activity toward a variety of substrates, including  $\rho$ -nitrophenyl acetate, organophosphorus compounds (OPs),  $\rho$ -naphthyl acetate, fatty acid esters, aspirin, and cyclophosphamide.<sup>45</sup>

**3.4.1. Effect of Functionalized Nanoplastics on Esterase Enzyme Activity.** The hydrolytic activity of albumin is commonly investigated using  $\rho$ -NPA, a standard substrate of carboxylesterase. By evaluating the synthesis of  $\rho$ -nitrophenol from the substrate  $\rho$ -nitrophenyl acetate, the esterase activity of HSA under the influence of various NPs was investigated in this experiment.  $\rho$ -Nitrophenol, a byproduct of  $\rho$ -NPA hydrolysis, is easily identifiable by spectrophotometry due to its yellow coloring and absorption peak at a wavelength of 400–412 nm.<sup>67</sup>

The esterase activity of HSA is shown in Figure 6a–c and Figure 9, in both its pure form and in combination with different functionalized NPs, such as PS, PS-COOH, and PS-NH<sub>2</sub>. The Michaelis–Menten plot clearly shows that all NPs decrease the esterase activity of HSA, with PS-NH<sub>2</sub> showing the greatest reduction. Table 2 contains enzyme kinetic parameters that were determined from the relevant Lineweaver–Burk plot (Figure 6d–f). Results from three separate studies were averaged, and the associated standard deviations were also provided. For the hydrolysis of  $\rho$ -NPA by pure HSA and NPs (0, 50, and 100  $\mu\text{g}/\text{mL}$ ) interacted HSA, the Michaelis–Menten constant ( $K_m$ ), maximal reaction velocity ( $V_{\text{max}}$ ), and catalytic constant ( $K_{\text{cat}}$ ) were calculated.

The potential mechanisms underlying the observed changes in esterase-like activity are as follows: In Sudlow site II, HSA's interaction with ester substrates takes place through specific amino acids such as Tyr-411, Tyr150, Tyr-138, Ser-193, and Lys-199, which are regarded as active site's catalytic amino acids, responsible for esterase activity of HSA.<sup>39,50,67</sup> These specific interactions are disturbed by HSA-nanoplastics interactions, as evidenced by enzyme assay results leading to changes in esterase activity.  $K_m$  values increased from  $1.1 \times 10^3$

to  $2.0 \times 10^3 \mu\text{M}$  for PS,  $1.1 \times 10^3$  to  $2.17 \times 10^3 \mu\text{M}$  for PS-COOH, and  $1.1 \times 10^3$  to  $2.50 \times 10^3 \mu\text{M}$  for PS-NH<sub>2</sub>; however,  $V_{\text{max}}$  values were even determined to be virtually constant. The increase in  $K_m$  values and consistent  $V_{\text{max}}$  values indicate that functionalized NPs are in a competitive race for the albumin's active site, which suggests that the manner of inhibition is also competitive. Competitive inhibition occurs when the substrate and the inhibitor bind in the same location (active site).  $V_{\text{max}}$  remains constant since raising the concentration of substrate counteracts the concentration of inhibitor. The reason for the rise in  $K_m$  is that more substrate is needed to reach maximal velocity in the presence of the inhibitor than it would be in the absence of the inhibitor.<sup>68</sup> Since all of the NPs and complexes engage in competitive binding, they all bind to the aforementioned residues or close by, preventing the substrate from attaching to HSA and decreasing its esterase activity, with the maximum effect being exhibited by PS-NH<sub>2</sub>. In agreement, the results of the fluorescence spectra demonstrate that all the NPs and complexes bind to HSA at aromatic fluorophore residues, including Tyr residues (Tyr-138, 150, 411 - a catalytic amino acid in esterase activity), as evidenced by quenching of fluorophores. The decrease in emission intensity by all the particles reveals the possible molecular interaction of NPs with fluorophores (especially Tyr) in the protein. Greater hypochromicity and blue shift in the PS-NH<sub>2</sub> spectra also correlate with the enzyme assay results, leading to greater structural changes and greater loss of esterase activity. The molecular interaction will be further supported by the results of CD spectra, where the alteration in the secondary structure of HSA by all the NPs, leads to the loss of  $\alpha$  helix and changes in Beta sheets, which further confirms the loss of functional activity of HSA with a maximum effect being exhibited by PS-NH<sub>2</sub>. In addition, molecular docking studies published in our previous research<sup>19,49</sup> also confirmed the molecular interaction of PSNPs and their pharmaceutical complex with HSA at the amino acids residues (Tyr-411, Tyr150, Tyr-138, Ser-193, and

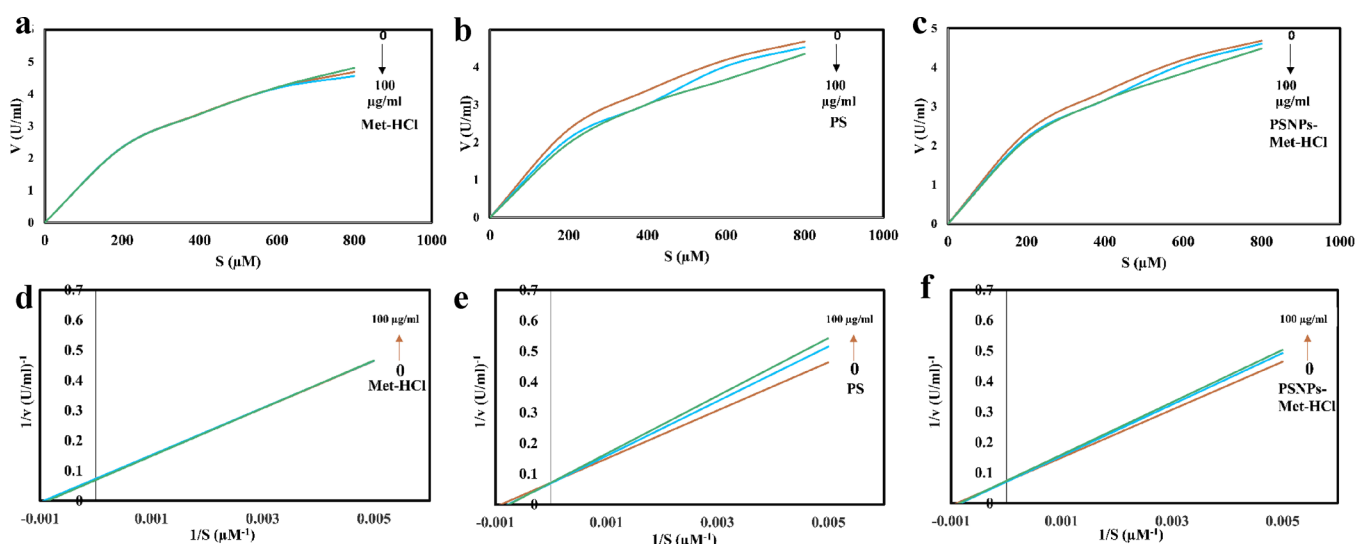


**Figure 8.** Michaelis–Menten plot: esterase enzyme activity of HSA on binding with (a) Met-HCl, (b) PS-500 nm, and (c) PSNPs-Met-HCl [NPs], 0, 50, and 100  $\mu\text{g/mL}$ . Lineweaver–Burk plot ( $\frac{1}{V}$  vs  $\frac{1}{S}$ ): (d) Met-HCl, (e) PS-500 nm, and (f) PSNPs-Met-HCl.

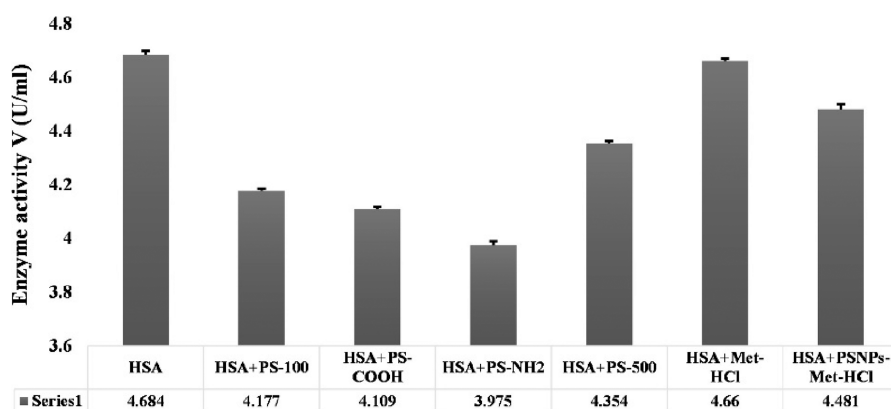


**Figure 9.** Esterase-like enzyme activity of HSA in the absence and presence of pollutants.  $[\rho\text{-NPA}]$  0–800  $\mu\text{M}$ , [NPs] 100  $\mu\text{g/mL}$ , [HSA]  $1 \times 10^{-5}$  M.

Lys-199), responsible for esterase activity. These interactions caused conformational changes and denaturation of protein, thereby decreasing esterase activity. The physiological function of HSA in the human body may be impacted in this way by structural alterations caused by pollutants. If the esterase activity of HSA is decreased by nanoplastics, from a drug point of view, medications entering the body containing ester substrates cannot be metabolized, leading to a decrease in their efficacy. Similarly, from a toxic substance's point of view, ester-containing toxic agents, (eg., organophosphates) entering the body cannot be hydrolyzed by HSA resulting in a decline in the detoxification process.

**3.4.2. Effect of Different Sized Nanoplastics on Esterase Enzyme Activity.** The results showed that NPs of various sizes can directly interact with HSA and reduce the activity of its esterase enzyme (Figure 7a,b and Figure 9) through competitive inhibition (Figure 7c,d). According to the Michaelis–Menten plot, 100 nm PS has a greater inhibitory effect on HSA's esterase activity than 500 nm PS. Although  $K_m$  values increased from  $1.1 \times 10^3$  to  $2.0 \times 10^3$   $\mu\text{M}$  for PS-100 nm and from  $1.1 \times 10^3$  to  $1.31 \times 10^3$   $\mu\text{M}$  for PS-500 nm, it was even found that  $V_{\text{max}}$  values were essentially stable (Table 2). The fact that  $K_m$  values are rising and  $V_{\text{max}}$  values remain stable

suggests that the inhibition is in competitive mode. The surface curvature of 100 nm PS was more favorable and caused a more noticeable shift in esterase activity.<sup>56</sup> This is consistent with the fluorescence spectra, which show that 100 nm NPs alter the polarity surrounding the tyrosine residue and decrease the endogenous fluorescence of HSA. Thus, smaller NPs have a greater impact on the structure and function of HSA due to their larger surface-to-volume ratio and greater surface reactivity with proteins. This property of reactivity with fluorophores/active site residues by competitive inhibition results in greater hypo/hypochromicity and increased esterase inhibition by 100 nm PS. Researchers have confirmed that smaller NPs have a greater impact on the structure and function of various proteins and enzymes (such as hemoglobin,<sup>56</sup> superoxide dismutase,<sup>61</sup> and catalase<sup>69</sup>), which is in accordance with the present findings.

**3.4.3. Effect of Pharmaceutical-Adsorbed Nanoplastics on Esterase Enzyme Activity.** The effect of pharmaceutical contaminant-adsorbed PSNPs on esterase enzyme activity (V) is shown in Figure 9 and as the MM plot in Figure 8c, compared with pure drug (Figure 8a) and pristine PS (Figure 8b). The MM plot clearly shows that the esterase activity of HSA was not inhibited by Met-HCl since they have negligible

binding affinity as found from fluorescence studies. Further pristine PSNPs decrease the enzyme activity higher than the PSNPs-Met-HCl complex. The type of inhibition exhibited by PSNPs and complexes (Figure 8d-f) is competitive since  $K_m$  values increased from  $1.1 \times 10^3$  to  $1.31 \times 10^3 \mu\text{M}$  for PS-500 nm and from  $1.1 \times 10^3$  to  $1.16 \times 10^3 \mu\text{M}$  for PSNPs-Met-HCl, also  $V_{\text{max}}$  values for both the ligands were approximately constant (Table 2). The mechanisms triggering the observed changes in esterase-like activity are as follows: since Met-HCl has negligible protein binding as evident from fluorescence studies, its interaction with HSA is not happening at the active site. Thus, the esterase activity of HSA was not disturbed by Met-HCl ( $V$  value of HSA+Met-HCl similar to that of HSA (Figure 9)). As explained before, pristine PSNPs bind competitively with HSA and reduce esterase activity, which is parallel to the results of fluorescence spectra (greater hypso and hypochromicity) and CD spectra. Coming to the PSNPs-Met-HCl complex, even though the binding is competitive, the negative impact on esterase activity is lesser than the impact of pristine PSNPs. This is due to the fact that Met-HCl covers the surface of PSNPs and reduces their competitive binding affinity with active sites, thus experiencing lesser impact on esterase activity. These results were coherent with the fluorescence and CD spectra results. Therefore, as explained before, when Met-HCl coats on the surface of PSNPs, drug reduces NP's binding affinity with protein, which might lead to direct transport of NPs to the target organs of Met-HCl such as liver, intestine, or kidney.<sup>70</sup> As a result, when nanoplastics are adsorbed with a pharmaceutical copollutant, their binding affinity with serum protein and influence on enzyme activity are dependent on the drug's binding affinity.

**3.5. Significance of HSA's Esterase Activity.** Human serum albumin (HSA) is the primary plasma protein with important roles as a depot and vector for numerous exogenous (drugs and harmful chemicals) proteins with significant metabolic activity. In terms of drug metabolism, aspirin is converted by HSA into salicylic acid, which is a critical step in the pharmacokinetics of aspirin.<sup>71</sup> This metabolism will be slowed if nanoplastics bind to HSA in a competitive manner. Like aspirin, many other medications lose their potency and effectiveness because of NPs. From a physiological perspective, the detoxifying character of ester-containing toxic substances is very significant due to the enormous volume of albumin in the blood plasma and the equilibrium nature of the interaction of numerous substrates with albumin. Detoxification of organophosphates, such as paraoxon, chlorpyrifos-oxon, and so forth by catalytic hydrolysis of HSA, was proved in the previous research. Cyanide compounds also get detoxified by HSA by binding to active site residues.<sup>39,72,73</sup> If the nanoplastics competitively bind with HSA, their detoxifying ability to the aforementioned or other toxic agents will be reduced if humans consume them. In toxicology, nanoplastic binding with HSA reduces the detoxification process and increases the bioaccumulation process.

## 4. CONCLUSIONS

Investigation of the modification of esterase-like activity of serum albumin by nanoplastics and their cocontaminants revealed the following conclusions: In terms of surface functionalization, amine-functionalized polystyrene nanoplastics induced greater hypochromicity and hypsochromicity in HSA than carboxy and pristine, demonstrating that amine groups induce greater structural alterations in HSA, which was

parallel to the CD spectral results. Smaller NPs have a bigger impact on HSA's structure than larger NPs do due to their larger surface area to volume ratio. Regarding copollutant-adsorbed NPs (pharmaceutical), Met-HCl lessens the effect of PSNPs on the conformational changes of HSA by lowering PSNPs' affinity for HSA, which was proved by both fluorescence and CD spectra. Hypochromicity in all of the fluorescence spectra portrays the surprising fact that all the pollutants interact with HSA or near the fluorophore site (especially Tyr), which is greatly involved in the active site for esterase activity. Enzyme assay studies proved that all of the pollutants bind with HSA by competitive inhibition except Met-HCl. These two results: competitive inhibition and binding at the fluorophores correlate well, revealing the mechanism behind inhibiting the esterase activity of HSA. While comparing the esterase activity of HSA in the presence of NPs, it was clarified that amine NPs inhibit esterase activity greater, smaller NPs impact esterase activity greater, and Met-HCl reduces the inhibiting effect of pristine PSNPs on esterase, since it covers the surface of PSNPs. Thus, Met-HCl may transport NPs to their target organs. Consequently, pharmaceutical pollutants can act as carriers for nanoplastic pollutants in the circulatory system, promoting their movement and accumulation in particular tissues. In conclusion, pollutants can attach to HSA and limit its esterase activity by competitive inhibition. These interactions may impair HSA's regular functioning leading to a negative impact on health. This study emphasizes the significance of measuring the esterase enzyme activity of serum albumin in order to understand the toxicokinetics and toxicodynamics of nanoplastics in the human body.

## AUTHOR INFORMATION

### Corresponding Author

Natarajan Chandrasekaran – Centre for Nanobiotechnology, Vellore Institute of Technology (VIT University), Vellore 632014 Tamil Nadu, India; [orcid.org/0000-0002-0586-134X](https://orcid.org/0000-0002-0586-134X); Phone: +91 416 2202624; Email: [nchandrasekaran@vit.ac.in](mailto:nchandrasekaran@vit.ac.in), [nchandra40@hotmail.com](mailto:nchandra40@hotmail.com); Fax: +91 416 2243092

### Author

Durgalakshmi Rajendran – Centre for Nanobiotechnology, Vellore Institute of Technology (VIT University), Vellore 632014 Tamil Nadu, India

Complete contact information is available at:

<https://pubs.acs.org/10.1021/acsomega.3c05447>

### Author Contributions

D.R. was responsible for investigation, methodology, data curation, writing the original draft and review, and editing. N.C. was responsible for conceptualization, supervision, resources, project administration, funding acquisition, writing the review, and editing.

### Notes

The authors declare no competing financial interest.

## ACKNOWLEDGMENTS

The authors express their gratitude to Indian Council of Medical Research (ICMR) for providing financial support through the Research Grant-F.No 36/2/2020/Toxi/BMS.

## ■ ABBREVIATIONS

HSA, human serum albumin  
PSNPs, polystyrene nanoplastics  
PS, pristine polystyrene nanoplastics  
PS-COOH, carboxylated polystyrene nanoplastics  
PS-NH<sub>2</sub>, aminated polystyrene nanoplastics  
Met-HCl, metformin hydrochloride  
PSNPs-Met-HCl, polystyrene nanoplastics adsorbed with metformin hydrochloride  
MM, Michaelis–Menten  
LB, Lineweaver–Burk  
IFESEM, field emission scanning electron microscopy  
 $\rho$ -NPA,  $\rho$ -nitrophenyl acetate  
 $\rho$ -NP,  $\rho$ -nitrophenol  
CD, circular dichroism

## ■ REFERENCES

- (1) Allen, S.; Allen, D.; Karbalaee, S.; Maselli, V.; Walker, T. R. Micro(Nano)Plastics Sources, Fate, and Effects: What We Know after Ten Years of Research. *J. Hazard. Mater. Adv.* **2022**, *6*, No. 100057.
- (2) Saeedi, M. How Microplastics Interact with Food Chain: A Short Overview of Fate and Impacts. *J. Food Sci. Technol.* **2023**, *1* DOI: 10.1007/s13197-023-05720-4.
- (3) Yu, Y.; Mo, W. Y.; Luukkonen, T. Adsorption Behaviour and Interaction of Organic Micropollutants with Nano and Microplastics – A Review. *Sci. Total Environ.* **2021**, *797*, No. 149140.
- (4) Gupta, C.; Kaushik, S.; Himanshu; Jain, S.; Dhanwani, I.; Mansi; Garg, S.; Paul, A.; Pant, P.; Gupta, N. Bioaccumulation and Toxicity of Polystyrene Nanoplastics on Marine and Terrestrial Organisms with Possible Remediation Strategies: A Review. *Environ. Adv.* **2022**, *8*, No. 100227.
- (5) Zhang, H.; Wang, J.; Zhou, B.; Zhou, Y.; Dai, Z.; Zhou, Q.; Christie, P.; Luo, Y. Enhanced Adsorption of Oxytetracycline to Weathered Microplastic Polystyrene: Kinetics, Isotherms and Influencing Factors. *Environ. Pollut.* **2018**, *243*, 1550–1557.
- (6) Liu, G.; Zhu, Z.; Yang, Y.; Sun, Y.; Yu, F.; Ma, J. Sorption Behavior and Mechanism of Hydrophilic Organic Chemicals to Virgin and Aged Microplastics in Freshwater and Seawater. *Environ. Pollut.* **2019**, *246*, 26–33.
- (7) Gong, W.; Jiang, M.; Han, P.; Liang, G.; Zhang, T.; Liu, G. Comparative Analysis on the Sorption Kinetics and Isotherms of Fipronil on Nondegradable and Biodegradable Microplastics. *Environ. Pollut.* **2019**, *254*, No. 112927.
- (8) Wang, T.; Yu, C.; Chu, Q.; Wang, F.; Lan, T.; Wang, J. Adsorption Behavior and Mechanism of Five Pesticides on Microplastics from Agricultural Polyethylene Films. *Chemosphere* **2020**, *244*, No. 125491.
- (9) Frias, J. P. G. L.; Sobral, P.; Ferreira, A. M. Organic Pollutants in Microplastics from Two Beaches of the Portuguese Coast. *Mar. Pollut. Bull.* **2010**, *60* (11), 1988–1992.
- (10) Mamtimin, X.; Song, W.; Wang, Y.; Habibul, N. Arsenic Adsorption by Carboxylate and Amino Modified Polystyrene Micro- and Nanoplastics: Kinetics and Mechanisms. *Environ. Sci. Pollut. Res.* **2023**, *30*, 44878.
- (11) Atugoda, T.; Vithanage, M.; Wijesekara, H.; Bolan, N.; Sarmah, A. K.; Bank, M. S.; You, S.; Ok, Y. S. Interactions between Microplastics, Pharmaceuticals and Personal Care Products: Implications for Vector Transport. *Environ. Int.* **2021**, *149*, No. 106367.
- (12) Fu, L.; Li, J.; Wang, G.; Luan, Y.; Dai, W. Adsorption Behavior of Organic Pollutants on Microplastics. *Ecotoxicol. Environ. Saf.* **2021**, *217*, No. 112207.
- (13) Elizalde-Velázquez, A.; Subbiah, S.; Anderson, T. A.; Green, M. J.; Zhao, X.; Cañas-Carrell, J. E. Sorption of Three Common Nonsteroidal Anti-Inflammatory Drugs (NSAIDs) to Microplastics. *Sci. Total Environ.* **2020**, *715*, No. 136974.
- (14) Xu, B.; Liu, F.; Brookes, P. C.; Xu, J. The Sorption Kinetics and Isotherms of Sulfamethoxazole with Polyethylene Microplastics. *Mar. Pollut. Bull.* **2018**, *131*, 191–196.
- (15) Liu, X.; Zheng, M.; Wang, L.; Ke, R.; Lou, Y.; Zhang, X.; Dong, X.; Zhang, Y. Sorption Behaviors of Tris-(2,3-Dibromopropyl) Isocyanurate and Hexabromocyclododecanes on Polypropylene Microplastics. *Mar. Pollut. Bull.* **2018**, *135*, 581–586.
- (16) Guo, X.; Pang, J.; Chen, S.; Jia, H. Sorption Properties of Tylosin on Four Different Microplastics. *Chemosphere* **2018**, *209*, 240–245.
- (17) Atugoda, T.; Wijesekara, H.; Werellagama, D. R. I. B.; Jinadasa, K. B. S. N.; Bolan, N. S.; Vithanage, M. Adsorptive Interaction of Antibiotic Ciprofloxacin on Polyethylene Microplastics: Implications for Vector Transport in Water. *Environ. Technol. Innovation* **2020**, *19*, No. 100971.
- (18) Bradley, P. M.; Journey, C. A.; Button, D. T.; Carlisle, D. M.; Clark, J. M.; Mahler, B. J.; Nakagaki, N.; Qi, S. L.; Waite, I. R.; VanMetre, P. C. Metformin and Other Pharmaceuticals Widespread in Wadeable Streams of the Southeastern United States. *Environ. Sci. Technol. Lett.* **2016**, *3* (6), 243–249.
- (19) Rajendran, D.; Varghese, R. P.; Doss, G. P.; Shivashankar, M.; Chandrasekaran, N. Interaction of Antidiabetic Formulation with Nanoplastics and Its Binary Influence on Plasma Protein. *Environ. Toxicol. Pharmacol.* **2023**, No. 104249.
- (20) Wang, W.; Wang, J. Comparative Evaluation of Sorption Kinetics and Isotherms of Pyrene onto Microplastics. *Chemosphere* **2018**, *193*, 567–573.
- (21) Zhang, Y. T.; Chen, H.; He, S.; Wang, F.; Liu, Y.; Chen, M.; Yao, G.; Huang, Y.; Chen, R.; Xie, L.; Mu, J. Subchronic Toxicity of Dietary Sulfamethazine and Nanoplastics in Marine Medaka (*Oryzias Melastigma*): Insights from the Gut Microbiota and Intestinal Oxidative Status. *Ecotoxicol. Environ. Saf.* **2021**, *226*, No. 112820.
- (22) Shi, W.; Han, Y.; Sun, S.; Tang, Y.; Zhou, W.; Du, X.; Liu, G. Immunotoxicities of Microplastics and Sertraline, Alone and in Combination, to a Bivalve Species: Size-Dependent Interaction and Potential Toxication Mechanism. *J. Hazard. Mater.* **2020**, *396*, No. 122603.
- (23) Zhang, S.; Ding, J.; Razanajatovo, R. M.; Jiang, H.; Zou, H.; Zhu, W. Interactive Effects of Polystyrene Microplastics and Roxithromycin on Bioaccumulation and Biochemical Status in the Freshwater Fish Red Tilapia (*Oreochromis Niloticus*). *Sci. Total Environ.* **2019**, *648*, 1431–1439.
- (24) Prata, J. C.; Lavorante, B. R. B. O.; Montenegro, M. da C. B.S.M.; Guilhermino, L. Influence of Microplastics on the Toxicity of the Pharmaceuticals Procainamide and Doxycycline on the Marine Microalgae *Tetraselmis Chuii*. *Aquatic Toxicology* **2018**, *197*, 143–152.
- (25) Wang, F.; Wang, B.; Qu, H.; Zhao, W.; Duan, L.; Zhang, Y.; Zhou, Y.; Yu, G. The Influence of Nanoplastics on the Toxic Effects, Bioaccumulation, Biodegradation and Enantioselectivity of Ibuprofen in Freshwater Algae *Chlorella Pyrenoidosa*. *Environ. Pollut.* **2020**, *263*, No. 114593.
- (26) Shi, X.; Xu, T.; Cui, W.; Qi, X.; Xu, S. Combined Negative Effects of Microplastics and Plasticizer DEHP: The Increased Release of Nets Delays Wound Healing in Mice. *Sci. Total Environ.* **2023**, *862*, No. 160861.
- (27) Zhong, G.; Rao, G.; Tang, L.; Wu, S.; Tang, Z.; Huang, R.; Ruan, Z.; Hu, L. Combined Effect of Arsenic and Polystyrene-Nanoplastics at Environmentally Relevant Concentrations in Mice Liver: Activation of Apoptosis, Pyroptosis and Excessive Autophagy. *Chemosphere* **2022**, *300*, No. 134566.
- (28) González-Fernández, C.; Díaz Baños, F. G.; Esteban, M. Á.; Cuesta, A. Functionalized Nanoplastics (NPs) Increase the Toxicity of Metals in Fish Cell Lines. *Int. J. Mol. Sci.* **2021**, *22* (13), 7141.
- (29) Almeida, M.; Martins, M. A.; Soares, A. M. V.; Cuesta, A.; Oliveira, M. Polystyrene Nanoplastics Alter the Cytotoxicity of Human Pharmaceuticals on Marine Fish Cell Lines. *Environ. Toxicol. Pharmacol.* **2019**, *69*, 57–65.

- (30) Kihara, S.; Van Der Heijden, N. J.; Seal, C. K.; Mata, J. P.; Whitten, A. E.; Köper, I.; McGillivray, D. J. Soft and Hard Interactions between Polystyrene Nanoplastics and Human Serum Albumin Protein Corona. *Bioconjugate Chem.* **2019**, *30* (4), 1067–1076.
- (31) Cao, J.; Yang, Q.; Jiang, J.; Dalu, T.; Kadushkin, A.; Singh, J.; Fakhruddin, R.; Wang, F.; Cai, X.; Li, R. Coronas of Micro/Nano Plastics: A Key Determinant in Their Risk Assessments. *Part. Fibre Toxicol.* **2022**, *19* (1), 55.
- (32) Gopinath, P. M.; Saranya, V.; Vijayakumar, S.; Mythili Meera, M.; Ruprekha, S.; Kunal, R.; Pranay, A.; Thomas, J.; Mukherjee, A.; Chandrasekaran, N. Assessment on Interactive Prospectives of Nanoplastics with Plasma Proteins and the Toxicological Impacts of Virgin, Coronated and Environmentally Released-Nanoplastics. *Sci. Rep.* **2019**, *9* (1), 8860.
- (33) Rabbani, G.; Lee, E. J.; Ahmad, K.; Baig, M. H.; Choi, I. Binding of Tolperisone Hydrochloride with Human Serum Albumin: Effects on the Conformation, Thermodynamics, and Activity of HSA. *Mol. Pharm.* **2018**, *15* (4), 1445–1456.
- (34) SUDLOW, G.; BIRKETT, D. J.; WADE, D. N. Further Characterization of Specific Drug Binding Sites on Human Serum Albumin. *Mol. Pharmacol.* **1976**, *12* (6), 1052–1061.
- (35) Rahman, S.; Rehman, M. T.; Rabbani, G.; Khan, P.; AlAjmi, M. F.; Hassan, Md. I.; Muteeb, G.; Kim, J. Insight of the Interaction between 2,4-Thiazolidinedione and Human Serum Albumin: A Spectroscopic, Thermodynamic and Molecular Docking Study. *Int. J. Mol. Sci.* **2019**, *20* (11), 2727.
- (36) Cedervall, T.; Lynch, I.; Lindman, S.; Berggård, T.; Thulin, E.; Nilsson, H.; Dawson, K. A.; Linse, S. Understanding the Nanoparticle-Protein Corona Using Methods to Quantify Exchange Rates and Affinities of Proteins for Nanoparticles. *Proc. Natl. Acad. Sci. U. S. A.* **2007**, *104* (7), 2050–2055.
- (37) Dix, K. J. Distribution and Pharmacokinetics. In *Hayes' Handbook of Pesticide Toxicology*; 2nd ed.; Krieger, R., Ed.; 2001; Elsevier, 2010; pp 923–939. DOI: 10.1016/B978-0-12-374367-1.00039-2.
- (38) Sekar, G.; Sugumar, S.; Mukherjee, A.; Chandrasekaran, N. Multiple Spectroscopic Studies of the Structural Conformational Changes of Human Serum Albumin - Essential Oil Based Nano-emulsions Conjugates. *J. Lumin.* **2015**, *161*, 187–197.
- (39) Goncharov, N. V.; Belinskaia, D. A.; Shmurak, V. I.; Terpilowski, M. A.; Jenkins, R. O.; Avdonin, P. V. Serum Albumin Binding and Esterase Activity: Mechanistic Interactions with Organophosphates. *Molecules* **2017**, *22* (7), 1201.
- (40) De Simone, G.; di Masi, A.; Ascenzi, P. Serum Albumin: A Multifaceted Enzyme. *Int. J. Mol. Sci.* **2021**, *22* (18), 10086.
- (41) Belinskaia, D. A.; Voronina, P. A.; Shmurak, V. I.; Jenkins, R. O.; Goncharov, N. V. Serum Albumin in Health and Disease: Esterase, Antioxidant, Transporting and Signaling Properties. *Int. J. Mol. Sci.* **2021**, *22* (19), 10318.
- (42) Liang, Z.; Sun, Y.; Zeng, H.; Qin, H.; Yang, R.; Qu, L.; Zhang, K.; Li, Z. Broad-Specificity Screening of Pyrethroids Enabled by the Catalytic Function of Human Serum Albumin on Coumarin Hydrolysis. *Anal. Chem.* **2023**, *95* (13), 5678–5686.
- (43) Yang, F.; Zhang, Y.; Liang, H. Interactive Association of Drugs Binding to Human Serum Albumin. *Int. J. Mol. Sci.* **2014**, *15*, 3580–3595.
- (44) Belinskaia, D. A.; Voronina, P. A.; Goncharov, N. V. Integrative Role of Albumin: Evolutionary, Biochemical and Pathophysiological Aspects. *J. Evol. Biochem. Physiol.* **2021**, *57* (6), 1419–1448.
- (45) Kragh-Hansen, U. Molecular and Practical Aspects of the Enzymatic Properties of Human Serum Albumin and of Albumin-Ligand Complexes. *Biochim. Biophys. Acta, Gen. Subj.* **2013**, *1830* (12), 5535–5544.
- (46) Ochs, R. S. Understanding Enzyme Inhibition. *J. Chem. Educ.* **2000**, *77* (11), 1453.
- (47) Ishtikhar, M.; Rabbani, G.; Khan, R. H. Interaction of 5-Fluoro-5'-Deoxyuridine with Human Serum Albumin under Physiological and Non-Physiological Condition: A Biophysical Investigation. *Colloids Surf., B* **2014**, *123*, 469–477.
- (48) Lakowicz, J. R. *Principles of Fluorescence Spectroscopy*; Springer, 2006.
- (49) Rajendran, D.; Chandrasekaran, N.; Waychal, Y.; Mukherjee, A. Nanoplastics Alter the Conformation and Activity of Human Serum Albumin. *NanoImpact* **2022**, *27*, No. 100412.
- (50) Zargar, S.; Wani, T. A. Exploring the Binding Mechanism and Adverse Toxic Effects of Persistent Organic Pollutant (Dicofol) to Human Serum Albumin: A Biophysical, Biochemical and Computational Approach. *Chem.-Biol. Interact.* **2021**, *350*, No. 109707.
- (51) Doran, P. M. Homogeneous Reactions. In *Bioprocess Engineering Principles*; Elsevier, 2013; pp 599–703. DOI: 10.1016/B978-0-12-220851-5.00012-5.
- (52) Jaya, R. P. Porous Concrete Pavement Containing Nanosilica from Black Rice Husk Ash. In *New Materials in Civil Engineering*; Elsevier, 2020; pp 493–527. DOI: 10.1016/B978-0-12-818961-0.00014-4.
- (53) Dimer, H. H.; Nichols, W. L.; Zimm, B. H.; Ten Eyck, L. F. Conformation-Invariant Structures of the A1 B1 Human Hemoglobin Dimer. *J. Mol. Biol.* **1997**, *270*, 598–615, DOI: 10.1006/jmbi.1997.1087.
- (54) Ghisaidoobe, A. B. T.; Chung, S. J. Intrinsic Tryptophan Fluorescence in the Detection and Analysis of Proteins: A Focus on Förster Resonance Energy Transfer Techniques. *Int. J. Mol. Sci.* **2014**, *5*, 22518–22538.
- (55) Artali, R.; Pra, A. Del; Foresti, E.; Lesci, I. G.; Roveri, N.; Sabatino, P. Adsorption of Human Serum Albumin on the Chrysotile Surface: A Molecular Dynamics and Spectroscopic Investigation. *J. R. Soc. Interface* **2008**, *5* (20), 273–283.
- (56) Zhao, Z.; Yao, J.; Li, H.; Lan, J.; Hollert, H.; Zhao, X. Interaction of Polystyrene Nanoplastics and Hemoglobin Is Determined by Both Particle Curvature and Available Surface Area. *Sci. Total Environ.* **2023**, *899*, No. 165617.
- (57) Rajendran, D.; Chandrasekaran, N. Molecular Interaction of Functionalized Nanoplastics with Human Hemoglobin. *J. Fluoresc.* **2023**, *1* DOI: 10.1007/s10895-023-03221-3.
- (58) Guglielmelli, A.; D'Aquila, P.; Palermo, G.; Dell'Aglio, M.; Passarino, G.; Strangi, G.; Bellizzi, D. Role of the Human Serum Albumin Protein Corona in the Antimicrobial and Photothermal Activity of Metallic Nanoparticles against *Escherichia Coli* Bacteria. *ACS Omega* **2023**, *8* (34), 31333–31343.
- (59) Vivian, J. T.; Callis, P. R. Mechanisms of Tryptophan Fluorescence Shifts in Proteins. *Biophys. J.* **2001**, *80* (5), 2093–2109.
- (60) Ju, P.; Zhang, Y.; Zheng, Y.; Gao, F.; Jiang, F.; Li, J.; Sun, C. Probing the Toxic Interactions between Polyvinyl Chloride Microplastics and Human Serum Albumin by Multispectroscopic Techniques. *Sci. Total Environ.* **2020**, *734*, No. 139219.
- (61) Wang, Y.; Shi, H.; Li, T.; Yu, L.; Qi, Y.; Tian, G.; He, F.; Li, X.; Sun, N.; Liu, R. Size-Dependent Effects of Nanoplastics on Structure and Function of Superoxide Dismutase. *Chemosphere* **2022**, *309*, No. 136768.
- (62) Shupe, H. J.; Boenisch, K. M.; Harper, B. J.; Brander, S. M.; Harper, S. L. Effect of Nanoplastic Type and Surface Chemistry on Particle Agglomeration over a Salinity Gradient. *Environ. Toxicol. Chem.* **2021**, *40* (7), 1820–1826.
- (63) Möller, M.; Denicola, A. Protein Tryptophan Accessibility Studied by Fluorescence Quenching. *Biochem. Mol. Biol. Educ.* **2002**, *30*, 175–178.
- (64) Paul, S.; Sepay, N.; Sarkar, S.; Roy, P.; Dasgupta, S.; Saha Sardar, P.; Majhi, A. Interaction of Serum Albumins with Fluorescent Ligand 4-Azido Coumarin: Spectroscopic Analysis and Molecular Docking Studies. *New J. Chem.* **2017**, *41* (24), 15392–15404.
- (65) Vignesh, G.; Manojkumar, Y.; Sugumar, K.; Arunachalam, S. Spectroscopic Investigation on the Interaction of Some Polymer-Cobalt(III) Complexes with Serum Albumins. *J. Lumin.* **2015**, *157*, 297–302.
- (66) Li, Z.; Zhao, L.; Sun, Q.; Gan, N.; Zhang, Q.; Yang, J.; Yi, B.; Liao, X.; Zhu, D.; Li, H. Study on the Interaction between 2,6-

Dihydroxybenzoic Acid Nicotine Salt and Human Serum Albumin by Multi-Spectroscopy and Molecular Dynamics Simulation. *Spectrochim. Acta, Part A* **2022**, *270*, No. 120868.

(67) Belinskaia, D. A.; Voronina, P. A.; Shmurak, V. I.; Jenkins, R. O.; Goncharov, N. V. Serum Albumin in Health and Disease: Esterase, Antioxidant, Transporting and Signaling Properties. *Int. J. Mol. Sci.* **2021**, *22*, 10318.

(68) Engelking, L. R. Enzyme Kinetics. In *Textbook of Veterinary Physiological Chemistry*; Elsevier, 2015; pp 32–38. DOI: [10.1016/B978-0-12-391909-0.50006-2](https://doi.org/10.1016/B978-0-12-391909-0.50006-2).

(69) Yao, J.; Li, H.; Lan, J.; Bao, Y.; Du, X.; Zhao, Z.; Hu, G. Spectroscopic Investigations on the Interaction between Nano Plastic and Catalase on Molecular Level. *Sci. Total Environ.* **2023**, *863*, No. 160903.

(70) Gong, L.; Goswami, S.; Giacomini, K. M.; Altman, R. B.; Klein, T. E. Metformin Pathways: Pharmacokinetics and Pharmacodynamics. *Pharmacogenet. Genomics* **2012**, *22* (11), 820–827.

(71) Yang, F.; Bian, C.; Zhu, L.; Zhao, G.; Huang, Z.; Huang, M. Effect of Human Serum Albumin on Drug Metabolism: Structural Evidence of Esterase Activity of Human Serum Albumin. *J. Struct. Biol.* **2007**, *157* (2), 348–355.

(72) Sogorb, M. A.; Vilanova, E. Enzymes Involved in the Detoxification of Organophosphorus, Carbamate and Pyrethroid Insecticides through Hydrolysis. *Toxicol. Lett.* **2002**, *128* (1–3), 215–228.

(73) Sogorb, M. A.; García-Argüelles, S.; Carrera, V.; Vilanova, E. Serum Albumin Is as Efficient as Paraxonase in the Detoxication of Paraoxon at Toxicologically Relevant Concentrations. *Chem. Res. Toxicol.* **2008**, *21* (8), 1524–1529.